Supplement of Earth Surf. Dynam., 7, 929–947, 2019
https://doi.org/10.5194/esurf-7-929-2019-supplement

Earth Surface Dynamics
Open Access
EGU

Supplement of

Reconstruction of river valley evolution before and after the emplacement of the giant Seymareh rock avalanche (Zagros Mts., Iran)

Michele Delchiaro et al.

Correspondence to: Michele Delchiaro (michele.delchiaro@uniroma1.it)

S1. The Zagros Fold-Thrust Belt, Tectonics and Seismicity

The Seymareh Landslide occurred in the latter tectonic domain, included between the High Zagros Fault (HZF) to the northeast and the Mountain Front Fault (MFF) to the southwest. The Simply Folded Belt involve in spectacular folds the 12–14 km thick sedimentary rocks of the Arabian margin succession covering the continental basement (e.g., McQuarrie, 2004 and references therein). The irregular geometry of the MFF that bounds the Simply Folded Belt southwestward from the Mesopotamian foreland basin, describes salients and reentrants (McQuarrie, 2004; Sepehr and Cosgrove, 2004): respectively, from northwest to southeast, the Pusht-e Kuh Arc (Lorestan), the Dezful Embayment, the Izeh Zone and the Fars Arc. A representative balanced cross-section of the Dezful embayment (Blanc et al., 2003) indicates ~49 km of shortening across the Simple Folded Zone. Homke et al., 2004 provide the dates of 8.1 and 7.2 Ma for the onset of the deformation in the front of the Push-e Kush Arc (related to the base of the growth strata observed in the NE flank of the Changuleh syncline) that lasted until 2.5 Ma, around the Pliocene–Pleistocene boundary. A long-term shortening rate of ~10 mm y^{-1} was derived for the deformation in the Simple Folded Zone, which is the same as the present-day one derived by GPS measurements (Tatar et al. 2002).

Seismicity is distributed in a 200-300 km wide area of the Zagros mountain range (Hatzfeld et al., 2010, Paul et al., 2010, Rajabi et al., 2011), with a sharp cut along the Main Zagros Reverse Fault in NE (e.g. Yamini-Fard et al., 2016). Looking at the depth and magnitude of recent earthquakes (Fig. S1), the seismogenic faults can generate recurrent earthquakes of Mw 5-6 and exceptional earthquakes of higher magnitude, i.e. up to Mw 6-8. These seismogenic faults follow the general trend of the Zagros, having NW-SE direction in the northwestern portion of the chain, while in the southeastern part they assume an E-W trend; they are characterized by high-angle planes (40-50°) reaching depths between 4 and 19 km (Hatzfeld et al., 2010; Paul et al., 2010, Rajabi et al., 2011). The earthquakes, which originate at a variable depth of 12-19 km, are probably located in the crystalline basement or at the interface with the Cambrian-Pliocene cover, whose thickness reaches about 12 km. The shallowest earthquakes, located at 4-8 km of depth, are located inside the sedimentary cover and, in general, these events do not produce surface ruptures, probably due to the presence of marly and evaporitic levels that accommodate the deformation (Hatzfeld et al., 2010; Leturmy and Robin, 2010; Navabpour et al., 2010; Paul et al., 2010; Saura et al., 2011).

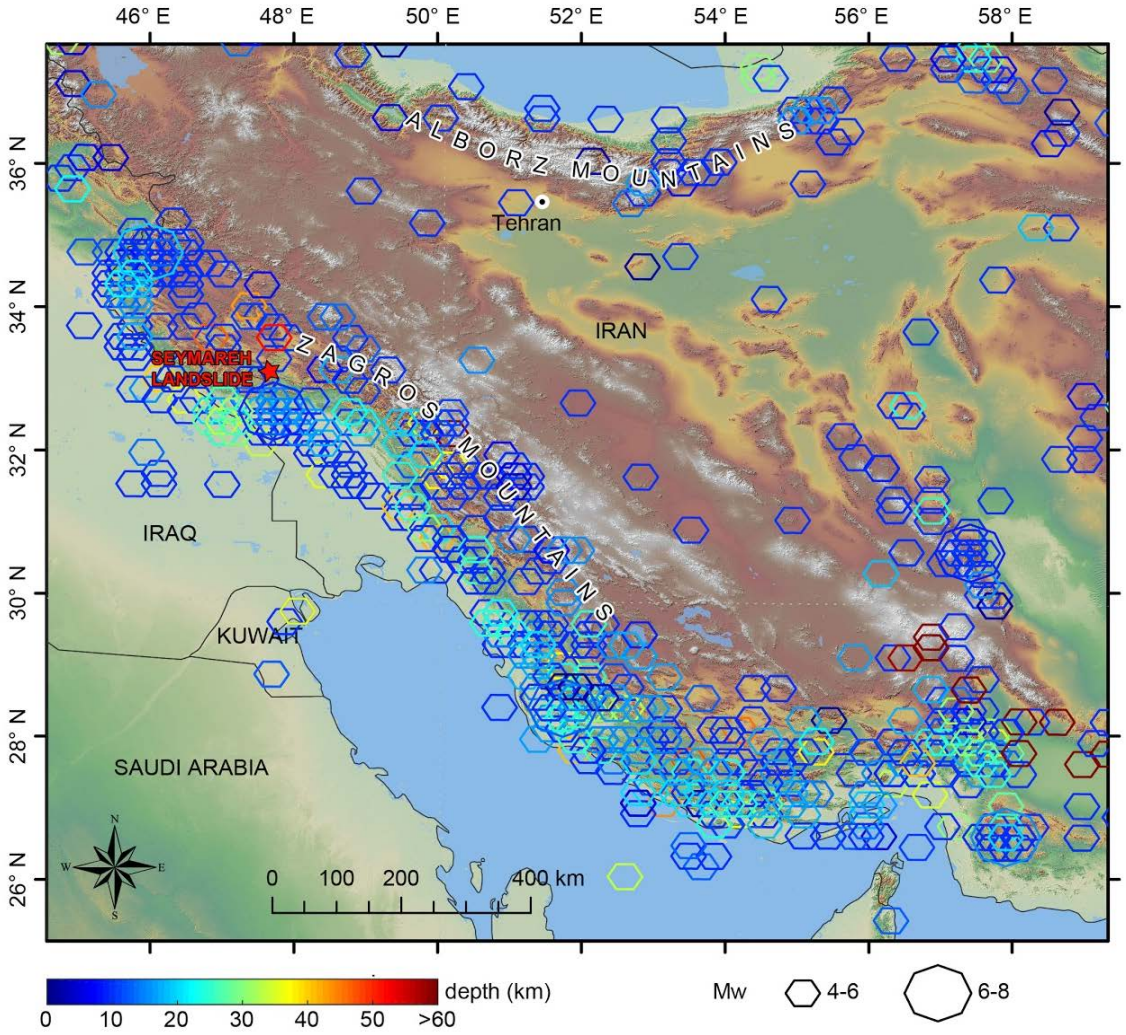

Figure. S1: Magnitude and depth of the recent earthquakes recorded in the Zagros Mountains (source: IRIS Earthquake Browser, https://www.iris.edu/hq/inclass/software-web-app/iris_earthquake_browser).

5

S2. OSL sample details

Sample No. **SEY3**

Sample Location (lat. and long required, country, state, county optional)

LAT: 32° 59.591'N; LONG: 47° 46.144'E – WESTERN IRAN

Sample depositional environment (e.g. eolian-medium sand, alluvial fan):

SANDY-GRAVELLY ALLUVIAL DEPOSIT. WE SAMPLED A SANDY LAYER

Stratigraphic and/or geomorphic context, sketch below (or attach photo):

TERRACED ALLUVIAL DEPOSIT (LEVEL 2 OF 4 – same terrace sequence of SEY10 and SEY11)

Estimate of burial moisture content:

The one expected for an alluvial deposit in arid climate

Elevation (meters above sea level)

485 m a.s.l.

Burial depth (meters from surface)

~ 1.5 m

Sample No. **SEY4**

Sample Location (lat. and long required, country, state, county optional)

LAT: 33° 13.197’N; LONG: 47° 18.382’E – WESTERN IRAN

Sample depositional environment (e.g. eolian-medium sand, alluvial fan):

VARVED LACUSTRINE DEPOSIT.

Stratigraphic and/or geomorphic context, sketch below (or attach photo):

Estimate of burial moisture content:

The one expected for a lacustrine deposit in arid climate

Elevation (meters above sea level)

590 m a.s.l.

Burial depth (meters from surface)

~ 25 m

Sample No. **SEY5**

Sample Location (lat. and long required, country, state, county optional)

LAT: 33° 13.437'N; LONG: 47° 18.219'E – WESTERN IRAN

Sample depositional environment (e.g. eolian-medium sand, alluvial fan):

ALLUVIAL PLAIN DEPOSIT. WE SAMPLED A SANDY LAYER.

Stratigraphic and/or geomorphic context, sketch below (or attach photo):

TERRACED ALLUVIAL DEPOSIT (LEVEL 1 OF 3 – same sequence of SEY6 and SEY8)

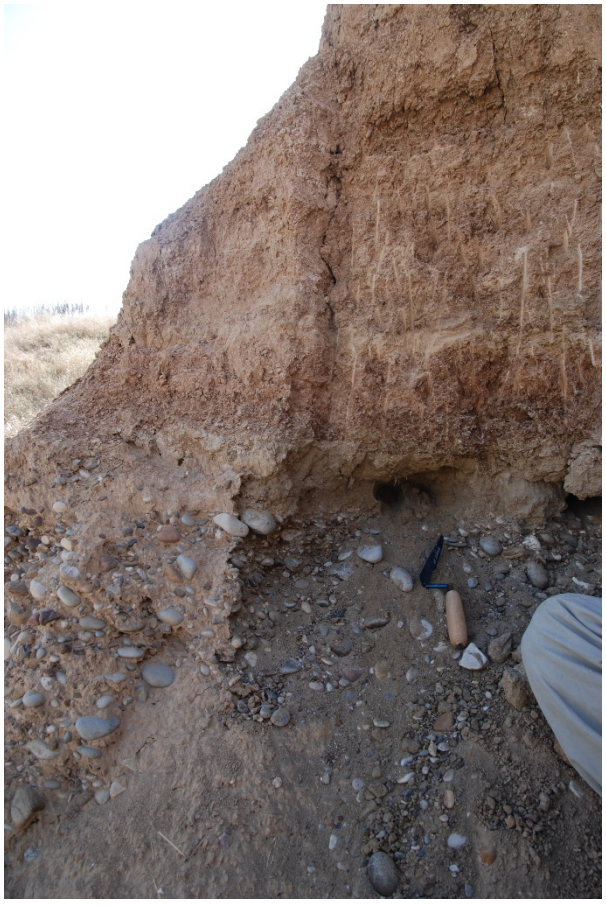

Estimate of burial moisture content:

The one expected for an alluvial deposit in arid climate

Elevation (meters above sea level)

607 m a.s.l.

Burial depth (meters from surface)

~ 1.5 m

Sample No. **SEY6**

Sample Location (lat. and long required, country, state, county optional)

LAT: 33° 13.291'N; LONG: 47° 18.358'E – WESTERN IRAN

Sample depositional environment (e.g. eolian-medium sand, alluvial fan):

ALLUVIAL PLAIN DEPOSIT. WE SAMPLED A SANDY LAYER.

Stratigraphic and/or geomorphic context, sketch below (or attach photo):

TERRACED ALLUVIAL DEPOSIT (LEVEL 3 OF 3 – same terrace sequence of SEY5 and SEY8)

Estimate of burial moisture content:

The one expected for an alluvial deposit in arid climate

Elevation (meters above sea level)

587 m a.s.l.

Burial depth (meters from surface)

~ 5 m

Sample No. **SEY8**

Sample Location (lat. and long required, country, state, county optional)

LAT: 33° 7.402'N; LONG: 47° 28.795'E – WESTERN IRAN

Sample depositional environment (e.g. eolian-medium sand, alluvial fan):

SANDY-GRAVELLY ALLUVIAL PLAIN DEPOSIT. WE SAMPLED A SANDY LAYER

Stratigraphic and/or geomorphic context, sketch below (or attach photo):

TERRACED ALLUVIAL DEPOSIT (LEVEL 2 OF 3 – same sequence of SEY5 and SEY6)

Estimate of burial moisture content:

The one expected for an alluvial deposit in arid climate

Elevation (meters above sea level)

561 m a.s.l.

Burial depth (meters from surface)

~ 2.5 m

Sample No. **SEY9**

Sample Location (lat. and long required, country, state, county optional)

LAT: 33° 4.462'N; LONG: 47° 34.197'E – WESTERN IRAN

Sample depositional environment (e.g. eolian-medium sand, alluvial fan):

SANDY-GRAVELLY ALLUVIAL DEPOSIT. WE SAMPLED A SANDY LAYER

Stratigraphic and/or geomorphic context, sketch below (or attach photo):

Estimate of burial moisture content:

The one expected for an alluvial deposit in arid climate

Elevation (meters above sea level)

570 m a.s.l.

Burial depth (meters from surface)

~ 1.5 m

Sample No. **SEY10**

Sample Location (lat. and long required, country, state, county optional)

LAT: 32° 59.335'N; LONG: 47° 46.071'E – WESTERN IRAN

Sample depositional environment (e.g. eolian-medium sand, alluvial fan):

SANDY-GRAVELLY-CONGLOMERATIC ALLUVIAL PLAIN DEPOSIT. WE SAMPLED A SANDY LAYER

Stratigraphic and/or geomorphic context, sketch below (or attach photo):

TERRACED ALLUVIAL DEPOSIT (LEVEL 3 OF 4 - same sequence as SEY3 and SEY11)

Estimate of burial moisture content:

The one expected for an alluvial deposit in arid climate

Elevation (meters above sea level)

436 m a.s.l.

Burial depth (meters from surface)

~ 2 m

Sample No. **SEY11**

Sample Location (lat. and long required, country, state, county optional)

LAT: 32° 59.265'N; LONG: 47° 45.869'E – WESTERN IRAN

Sample depositional environment (e.g. eolian-medium sand, alluvial fan):

SANDY-GRAVELLY-CONGLOMERATIC ALLUVIAL PLAIN DEPOSIT. WE SAMPLED A SANDY LAYER

Stratigraphic and/or geomorphic context, sketch below (or attach photo):

TERRACED ALLUVIAL DEPOSIT (LEVEL 4 OF 4 - same sequence as SEY3 and SEY10)

Estimate of burial moisture content:

The one expected for an alluvial deposit in arid climate

Elevation (meters above sea level)

400 m a.s.l.

Burial depth (meters from surface)

~ 1 m

References

Blanc, E. J.-P., Allen, M. B., Inger, S. and Hassani, H.: Structural styles in the Zagros Simple Folded Zone, Iran, J. Geol. Soc. London, 160Bisbal, 401–412. Available from: Blanc_et_al_2003.pdf, 2003.

Hatzfeld, D., Authemayou, C., Van der Beek, P., Bellier, O., Lavé, J., Oveisi, B., Tatar, M., Tavakoli, F., Walpersdorf, A. and Yamini-Fard, F.: The kinematics of the Zagros Mountains (Iran), Geol. Soc. London, Spec. Publ., 330(1), 19–42, doi:10.1144/SP330.3, 2010.

Homke, S., Vergés, J., Garcés, M., Emami, H. and Karpuz, R.: Magnetostratigraphy of Miocene-Pliocene Zagros foreland deposits in the front of the Push-e Kush Arc (Lurestan Province, Iran), Earth Planet. Sci. Lett., 225(3–4), 397–410, doi:10.1016/j.epsl.2004.07.002, 2004.

Leturmy, P. and Robin, C.: Tectonic and stratigraphic evolution of Zagros and Makran during the Mesozoic-Cenozoic: introduction, Geol. Soc. London, Spec. Publ., 330(1), 1–4, doi:10.1144/SP330.1, 2010.

McQuarrie, N.: Crustal scale geometry of the Zagros fold-thrust belt, Iran, J. Struct. Geol., 26(3), 519–535, doi:10.1016/j.jsg.2003.08.009, 2004.

Navabpour, P., Angelier, J. and Barrier, E.: Mesozoic extensional brittle tectonics of the Arabian passive margin, inverted in the Zagros collision (Iran, interior Fars), Geol. Soc. London, Spec. Publ., 330(1), 65-96, doi:10.1144/SP330.5, 2010.

Paul, A., Hatzfeld, D., Kaviani, A., Tatar, M. and Péquegnat, C.: Seismic imaging of the lithospheric structure of the Zagros mountain belt (Iran), Geol. Soc. London, Spec. Publ., 330(1), 5–18, doi:10.1144/SP330.2, 2010.

Rajabi, A. M., Mahdavifar, M. R., Khamehchiyan, M. and del Gaudio, V.: A new empirical estimator of coseismic landslide displacement for Zagros Mountain region (Iran), Nat. Hazards, 59(2), 1189–1203, doi:10.1007/s11069-011-9829-1, 2011.

Saura, E., Verges, J., Homke, S., Blanc, E., Serra-Kiel, J., Bernaola, G., Casciello, E., Fernandez, N., Romaire, I., Casini, G., Embry, J. C., Sharp, I. R. and Hunt, D. W.: Basin architecture and growth folding of the NW Zagros early foreland basin during the Late Cretaceous and early Tertiary, J. Geol. Soc. London., 168(1), 235–250, doi:10.1111/j.1601-5037.2004.00096.x, 2011.

Sepehr, M. and Cosgrove, J. W.: Structural framework of the Zagros Fold-Thrust Belt, Iran, Mar. Pet. Geol., 21(7), 829–843, doi:10.1016/j.marpetgeo.2003.07.006, 2004.

Tatar, M., Hatzfeld, D., Martinod, J., Walpersdorf, A., Ghafori-Ashtiany, M. and Chéry, J.: The present-day deformation of the central Zagros from GPS measurements, Geophys. Res. Lett., 29(19), 33-1-33–4, doi:10.1029/2002GL015427, 2002.

Yamini-Fard, F., Hatzfeld, D., Tatar, M. and Mokhtari, M.: Microearthquake seismicity at the intersection between the Kazerun fault and the Main Recent Fault (Zagros, Iran), Geophys. J. Int., 166(1), 186-196, doi:10.1111/j.1365-246X.2006.02891.x, 2006.